Underpredicted ENSO Teleconnections in Seasonal Forecasts

Ned C Williams[1], Adam A. Scaife[2], and James A Screen[1]

[1]University of Exeter
[2]Met Office Hadley Centre

January 20, 2023

Abstract

The El Niño-Southern Oscillation (ENSO) influences climate variability across the globe. ENSO is highly predictable on seasonal timescales and therefore its teleconnections are a source of extratropical forecast skill. To fully harness this predictability, teleconnections must be represented accurately in seasonal forecasts. We find that a multimodel ensemble from five seasonal forecast systems can successfully capture the spatial structure of the late winter (JFM) El Niño teleconnection to the North Atlantic via North America, but the simulated amplitude is half of that observed. We find that weak amplitude teleconnections exist in all five models and throughout the troposphere, and that the La Niña teleconnection is also weak. We find evidence that the tropical forcing of the teleconnection is not underestimated and instead, deficiencies are likely to emerge in the extratropics. We investigate the impact of underestimated teleconnection strength on North Atlantic winter predictability, including its relevance to the signal-to-noise paradox.

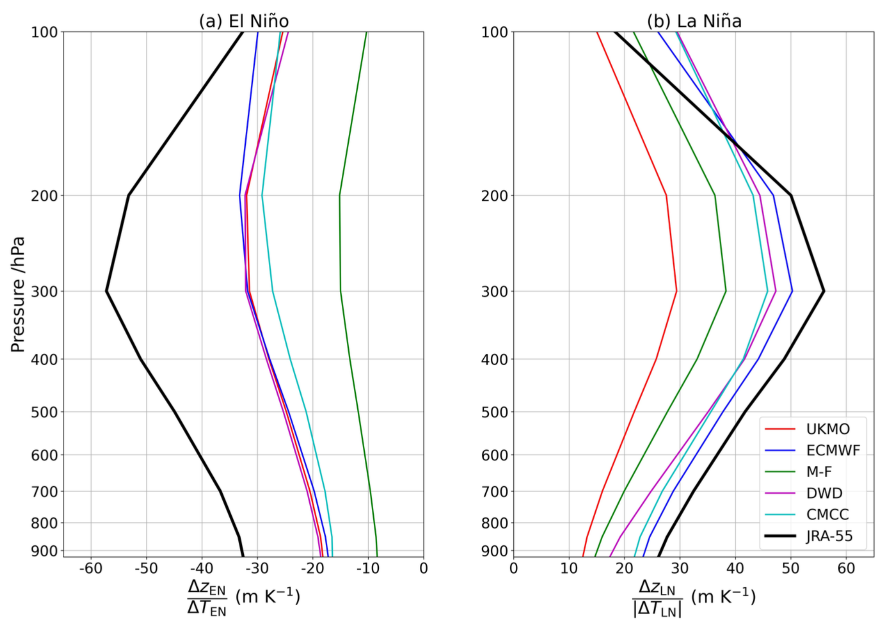

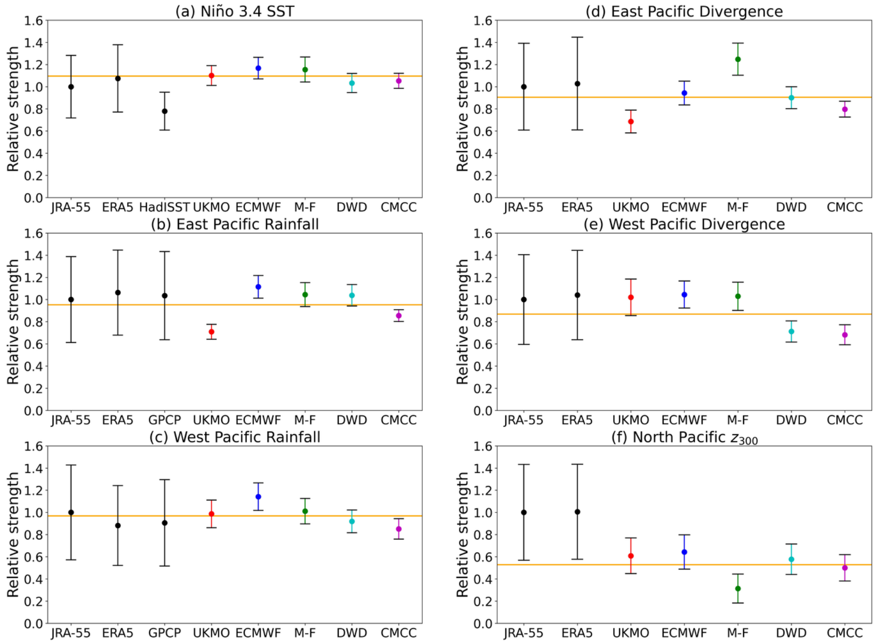
(a) Niño 3.4 SST
(b) East Pacific Rainfall
(c) West Pacific Rainfall
(d) East Pacific Divergence
(e) West Pacific Divergence
(f) North Pacific z_{300}
Relative strength
JRA-55
ERA5
HadISST
GPCP
UKMO
ECMWF
M-F
DWD
CMCC

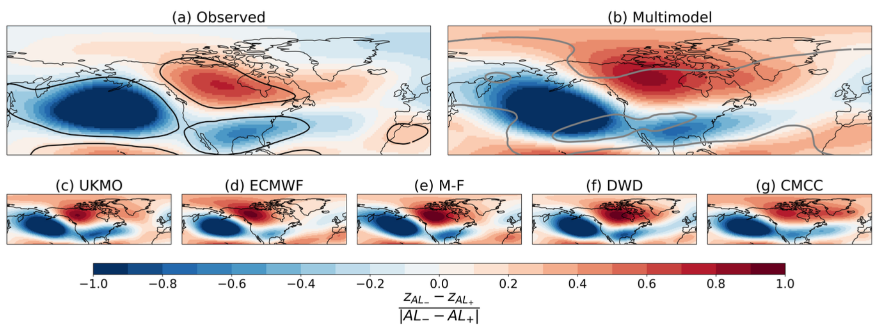
(a) Observed
(b) Multimodel
(c) UKMO
(d) ECMWF
(e) M-F
(f) DWD
(g) CMCC
$\frac{z_{AL_-} - z_{AL_+}}{|AL_- - AL_+|}$

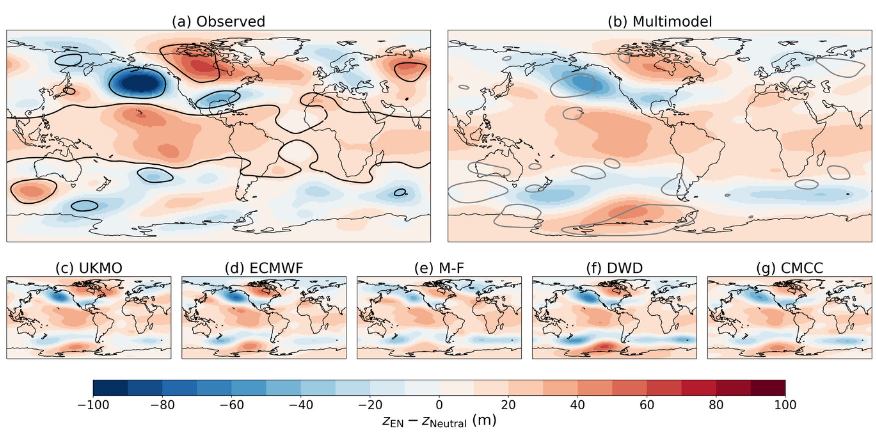
(a) Observed
(b) Multimodel
(c) UKMO
(d) ECMWF
(e) M-F
(f) DWD
(g) CMCC
$z_{\mathrm{EN}} - z_{\mathrm{Neutral}}$ (m)

Underpredicted ENSO Teleconnections in Seasonal Forecasts

N. C. Williams[1], A. A. Scaife[1,2], and J. A. Screen[1]

[1]Faculty of Environment, Science and Economy, University of Exeter, Exeter, UK
[2]Met Office Hadley Centre, Exeter, UK

Key Points:

- Seasonal forecasts severely underestimate the response to ENSO in the extratropical North Pacific
- The underestimated model response exists throughout the troposphere and is present for both El Niño and La Niña
- Tropical processes which generate the teleconnection are well predicted and so the problem does not appear to originate in the deep tropics

Corresponding author: Ned Williams, nw432@exeter.ac.uk

Abstract

The El Niño-Southern Oscillation (ENSO) influences climate variability across the globe. ENSO is highly predictable on seasonal timescales and therefore its teleconnections are a source of extratropical forecast skill. To fully harness this predictability, teleconnections must be represented accurately in seasonal forecasts. We find that a multimodel ensemble from five seasonal forecast systems can successfully capture the spatial structure of the late winter (JFM) El Niño teleconnection to the North Atlantic via North America, but the simulated amplitude is half of that observed. We find that weak amplitude teleconnections exist in all five models and throughout the troposphere, and that the La Niña teleconnection is also weak. We find evidence that the tropical forcing of the teleconnection is not underestimated and instead, deficiencies are likely to emerge in the extratropics. We investigate the impact of underestimated teleconnection strength on North Atlantic winter predictability, including its relevance to the signal-to-noise paradox.

Plain Language Summary

The El Niño-Southern Oscillation (ENSO) describes the cycle of warmer and cooler sea surface temperatures in the tropical Pacific Ocean, which influences climate around the globe. The high heat capacity of the ocean means that ENSO changes relatively slowly and so the ENSO phase — known as El Niño or La Niña — can be predicted with high accuracy several months ahead. Far-flung influences — known as teleconnections — of ENSO can provide predictability away from the tropics in seasonal forecasts if they are accurately modelled. In this work, the late winter (Jan–Mar) ENSO teleconnection to the North Atlantic, which travels via the North Pacific and North America, is investigated in five forecast models. We find that in all five models, the pattern of the teleconnection is accurately captured, but the strength of the modelled teleconnection is half of that in the real world. We find that the strength of processes in the tropics which cause the teleconnection — including changes in sea surface temperatures and rainfall — are not underestimated by models, meaning that the problem arises further along the pathway to the extratropics. This error likely contributes to the currently unresolved 'signal to noise paradox' in climate forecasts.

1 Introduction

The El Niño-Southern Oscillation (ENSO) is a major driver of global climate on interannual timescales. Sea surface temperature anomalies associated with ENSO lead to shifts in tropical convection, which generate poleward propagating Rossby waves (Sardeshmukh & Hoskins, 1988). This leads to a quasi-stationary wave response in the extratropics, which is modulated by the annual cycle. During the warm El Niño phase, a negative pressure anomaly persists in the North Pacific throughout the winter, with a positive anomaly over western Canada (Horel & Wallace, 1981). The response in the North Atlantic is typically strongest in late winter and resembles the negative phase of the North Atlantic Oscillation (Moron & Gouirand, 2003; Ayarzagüena et al., 2018). The Aleutian Low, which is strongly coupled to ENSO, has been shown to have an inverse relationship with the North Atlantic Oscillation in late winter (Honda et al., 2001). Several causes of the intraseasonal change in the teleconnection to the North Atlantic have been suggested, including modulation by the stratosphere (Ineson & Scaife, 2009; Cagnazzo & Manzini, 2009), and by differences in the tropical convective response in the west Pacific (Bladé et al., 2008) and in the Indian Ocean (Abid et al., 2021).

In seasonal forecasts, ENSO is a potential source of predictability as it varies on longer than seasonal timescales. In order to translate this potential predictability into true predictability, models need to accurately capture teleconnections from ENSO to the extratropics. Not all variability in the climate system is predictable, but ideally models should capture the fraction of variance which is predictable. However, seasonal forecasts have been found to underestimate this fraction in predictions of the North Atlantic Oscillation (Eade et al., 2014; Scaife et al., 2014; Baker et al., 2018). This phenomenon is known as the signal-to-noise paradox (Scaife & Smith, 2018), as it is associated with an underestimated signal-to-noise ratio, and counter-intuitively implies that models are better at predicting the real world than they are at predicting their own ensemble members.

Whilst there is extensive literature on the winter extratropical response to ENSO in observations and free-running GCMs, existing literature on modelled amplitude of the extratropical response, or the performance of seasonal forecasts in capturing the response is relatively limited. Very few studies have used multimodel forecasts to examine their representation of ENSO-extratropical teleconnections (e.g. L'Heureux et al. (2017)).

We investigate the performance of five seasonal forecast systems in capturing teleconnections from ENSO to the North Pacific, North America and the the North Atlantic. We then seek to establish the region in which teleconnection errors originate. We then further examine the North Pacific–North Atlantic teleconnection pathway (cf. Honda et al. (2001)) in order to understand the effect of errors in modelled teleconnections on North Atlantic predictability in the context of the signal-to-noise paradox.

2 Data and Methods

We use hindcasts for the winters 1993/1994 to 2016/2017 from five seasonal forecast systems. Met Office GloSea5 (MacLachlan et al. (2015); hereafter UKMO) hindcasts have 21 members, with 7 each initialized on the 25th October, 1st November and 8th November. Météo-France System 8 (Voldoire et al. (2019); M-F) hindcasts have 25 members, with 1 initialized on the 1st November, 12 initialized on the last Thursday of October, and 12 initialized on the penultimate Thursday of October. CMCC-SPS3 (Sanna et al. (2016); CMCC), DWD GCFS 2 (Fröhlich et al. (2021); DWD) and ECMWF SEAS5 (Johnson et al. (2019); ECMWF) hindcasts respectively have 40, 30 and 25 members initialized on the 1st November. Where multimodel means have been computed, ensemble members are weighted equally, although results are robust to equal weighting of models (not shown). The JRA-55 (Kobayashi et al., 2015) reanalysis with data from 1979/80–2016/17 is used for observations, and the ERA5 (Hersbach et al., 2020) reanalysis with the same period is used for comparison. Additionally, the Global Precipitation Climatology Project v2.3 (Adler et al. (2003); hereafter GPCP) observational dataset from 1979/1980-2016/2017 is also used for precipitation, and the HadISST 2.2 dataset (Kennedy et al. (2017); hereafter HadISST) from 1950/51-2014/15 is also used for sea surface temperatures. For sea surface temperatures, December–March (DJFM) means are used. For all other fields, January–March (JFM) means are used. Late winter is the focus of this work as the North Atlantic response to ENSO is most robust during this period (Moron & Gouirand, 2003).

The Niño 3.4 index (Trenberth, 1997) — defined as the mean SST anomaly ΔT between 190–240°E and 5°S–5°N — is computed for the JRA-55 reanalysis and is used to split winters into El Niño ($\Delta T > 0.5$ K), La Niña ($\Delta T < -0.5$ K) and neutral ($|\Delta T| < 0.5$ K) phases. Of the 24 hindcast winters, 6 are classified as El Niño, 9 as La Niña, and 9 as neutral. The 38 winters in the reanalysis period consist of 10 El Niño, 11 La Niña and 17 neutral seasons. Hindcast Niño 3.4 indices correlate strongly with observations (r is between 0.96 and 0.99 for the ensemble mean of each model).

For a given field, the response to El Niño is defined as the composite mean of El Niño years for that field with the neutral composite subtracted. Similarly, the response to La Niña is the La Niña composite with neutral subtracted. For the purpose of quantifying uncertainty, standard deviations for observed El Niño responses are computed as the standard deviation of all El Niño years for the relevant dataset. In order to compare model standard deviations with observations, a sampling technique is used. For each sample, a neutral mean is computed using a random member from each neutral year. This is then subtracted from a random ensemble member from an El Niño year. 10,000 samples are taken, for which the standard deviation is computed.

Tropical East Pacific precipitation (TEP) is defined as the mean precipitation between 160–240°E and 5°S–5°N, and is strongly coupled to ENSO. Tropical West Pacific precipitation (TWP) is defined as the mean precipitation between 110–150°E and 0–20°N. These boxes were chosen to capture the strongest precipitation responses during both El Niño and La Niña years, and are similar to the TEP and TWP boxes used in Scaife et al. (2017). TWP is considered as it has a known impact on the extratropical Northern Hemisphere, including the North Atlantic Oscillation (Kucharski et al., 2006; Scaife et al., 2017; Scaife, Ferranti, et al., 2019).

Due to the observed asymmetry of the North Pacific response to El Niño and La Niña, boxed regions of 180–220°E and 40–60°N for El Niño, and 170–210°E and 30–50°N for La Niña, are used when comparing the strength of the extratropical responses. These boxes are chosen in order to capture the strongest response in each phase.

The Aleutian Low is defined as the mean 300 hPa geopotential height z between 170–220°E and 30–60°N. This is a region of climatological low geopotential height with high interannual variability, and the boundaries are chosen to capture the regions with the strongest responses during El Niño and La Niña years. Aleutian Low composites are taken by defining negative and positive phases, where the Aleutian Low is deeper (more negative) or shallower (less negative) than the mean respectively. As the correlation between models and observation is less strong for the Aleutian Low than it is for the Niño 3.4 index ($0.5 < r < 0.7$ for the ensemble mean of models), model Aleutian Low indices are used to create model composites instead of the observed index. The 38 reanalysis winters consist of 17 negative seasons and 21 positive seasons. The multimodel ensemble mean evenly splits into 12 negative and 12 positive winters. DWD has 11 negative winters out of 24, UKMO and M-F both have 12, and ECMWF and CMCC both have 14.

3 Weak Teleconnections

Figure 1 (a) shows the response of 300 hPa geopotential height to El Niño computed using JRA-55 data. A significant increase in geopotential height occurs throughout most of the tropics due to tropical warming and the canonical Pacific-North American pattern (e.g. Horel and Wallace (1981)) is present. In the North Atlantic a tripole pattern emerges, with a large positive anomaly across the basin just south of Greenland, and negative anomalies to the north east and south west.

Figure 1 (b) shows the multimodel response to El Niño. The simulated pattern is very similar to that observed but the strength of the response in the extratropical Northern Hemisphere is severely underestimated. This is most evident over the North Pacific, where the magnitude of the composite response is greater than 90 m over a large region in observations but does not exceed 60 m anywhere in the multimodel mean. Figure 1 (c)–(g) shows the individual model responses. Each model captures the structure of the response over the North Pacific and North America, and all except the Météo-France model show a North Atlantic pattern which resembles the observed pattern. The underestimated amplitude of the teleconnection is present in all five models. Additionally, in all models the North Pacific response is tilted on a north west–south east axis relative to observations. Whilst the response over North America appears to be weak, significance is lower than in the North Pacific.

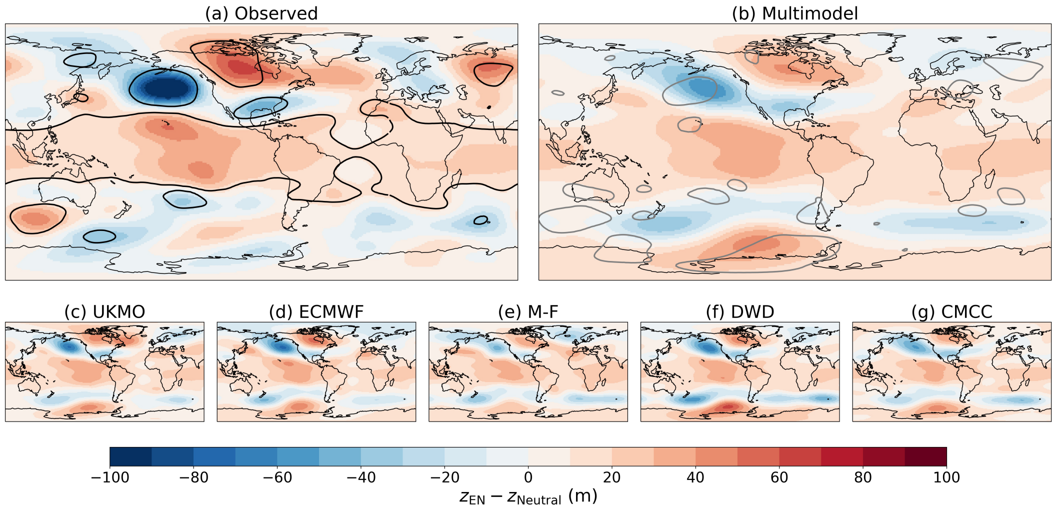

Figure 1. El Niño teleconnections in observations and models. Difference between El Niño and neutral composites of 300 hPa geopotential height for JRA-55 (a), the mean of all five models (b) and each of the five models ((c)–(g), labelled). Black line contours on (a) bound regions where the El Niño and neutral years are significantly different above the 10% level in observations according to a two-tailed t test. Gray line contours on (b) bound regions where the modelled response is significantly different to the observed response at the 10% level according to a two-tailed t test.

While there is reasonable agreement between observed and modelled teleconnections in the North Atlantic, the observed North Atlantic pattern for this period closely resembles the Atlantic wavetrain response to strong El Niño events found in Toniazzo and Scaife (2006). Removing the four El Niño events (1983, 1992, 1998, 2016) classed as strong by their definition ($\Delta T > 1.5$ K) from the observed composite leads to a pattern which more closely resembles the pattern from the multimodel mean (not shown). This may mean that either the models do not capture the non-linearity in the North Atlantic response, or that part of the strong El Niño pathway via the tropical Atlantic found in Toniazzo and Scaife (2006) is also too weak. However, the limited availability of observed El Niño years means that caution should be taken when comparing strength-based subsamples of the available data.

Figure 2 (a) shows that the extratropical Pacific response to El Niño is underestimated throughout the troposphere and in all five models, by about half in four models and even more than this in M-F. Figure 2 (b) shows that the response to La Niña is also underestimated in all models, at all tropospheric levels except for 100 hPa. The modelled El Niño and La Niña responses are not equally weak, with a less weak response to La Niña in most models. For this reason, we focus on the response to El Niño in the next section. Figure S1 shows maps of the 300 hPa geopotential height response to La Niña, calculated using JRA-55 (a) and the multimodel ensemble mean (b). The peak strength of the response to La Niña in the North Pacific is strongly underestimated in the multimodel mean, but the spatial extent of the positive geopotential height anomaly is broader than observed.

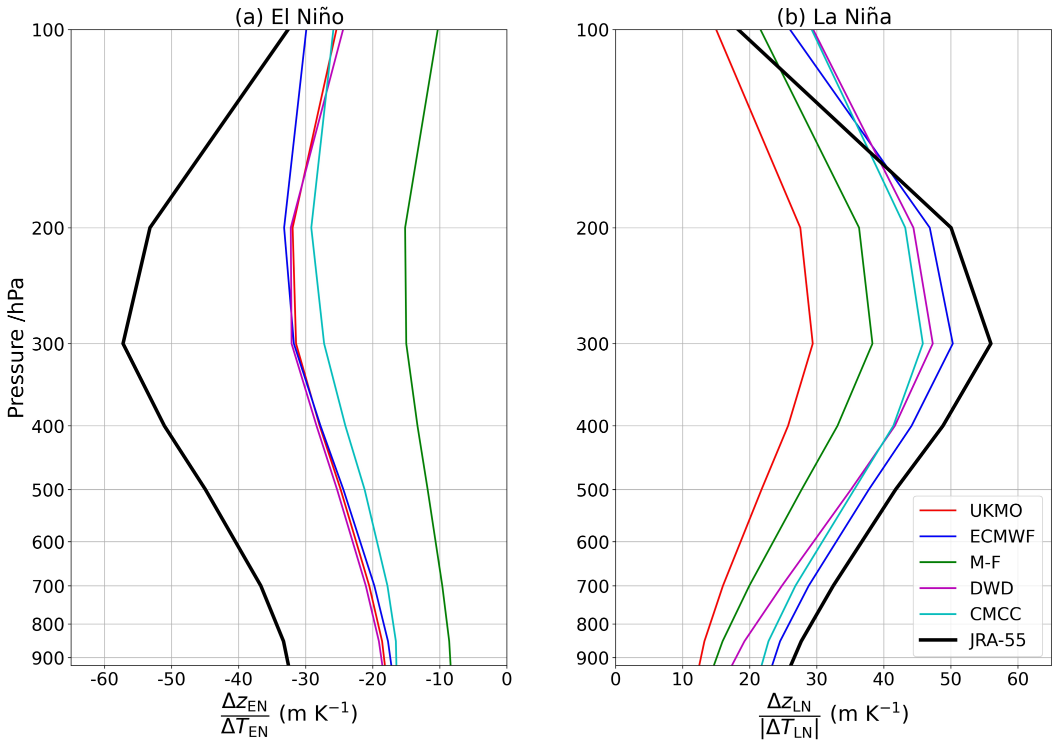

Figure 2. Vertical structure of ENSO teleconnections to the North Pacific. Different boxes are used for the two phases — (180–220°E, 40–60°N) for El Niño and (170–210°E, 30–50°N) for La Niña — to account for asymmetry in the teleconnection. The geopotential height responses are divided by the Niño 3.4 index response from the same source to account for SST biases.

4 Errors in the Teleconnection Pathway

We next consider where the model errors emerge in the chain of processes involved in the teleconnection. Figure 3 shows the strength of the response of six indices to El Niño in observational datasets and in hindcasts, with $\pm$ two standard errors from the mean shown to represent uncertainty. Figure 3 (a) shows that all five models actually *overestimate* changes in Niño 3.4 sea surface temperatures relative to JRA-55, although the model means are within the uncertainty range. This suggests that if sea surface temperatures were perfectly predicted, the underestimation of the modelled teleconnection would be even worse. When comparing to ERA5, there is almost no error in the multimodel mean response. All five models are above the uncertainty range of HadISST, although it should be noted that the HadISST time period (1950/51–2014/15) is different to the reanalysis period. Modelled responses of East Pacific (TEP) rainfall to El Niño (Figure 3 (b)) are similar to those in JRA-55, with two models underestimating the response and three models overestimating, and the difference between the JRA-55 and multimodel mean is much smaller than their respective uncertainties. ERA5 and GPCP are in strong agreement with JRA-55 for the TEP response to El Niño. For West Pacific (TWP) rainfall (Figure 3 (c)) all three observational datasets and all five models show similar responses, with model responses well within the uncertainty range of each observational dataset.

The generation of Rossby waves requires a Rossby wave source S (Sardeshmukh & Hoskins, 1988)

$$S = -\zeta \boldsymbol{\nabla} \cdot \boldsymbol{u}_\chi - \boldsymbol{u}_\chi \cdot \boldsymbol{\nabla} \zeta, \tag{1}$$

where ζ is the absolute vorticity and $\boldsymbol{u}_\chi$ is the divergent component of the horizontal wind. Increased tropical precipitation due to surface heating is associated with a baroclinic divergence response, with convergence near the surface and divergence at the level of convective outflow. Tropical divergence anomalies lead to divergent winds over a broader region, extending into areas with higher background vorticity and more favourable conditions for Rossby wave propagation. We found that the divergence response to ENSO in the tropical Pacific is not robust at 300 hPa, but it is highly robust and strongly correlated with precipitation at 200 hPa. This level is consistent with previous studies (e.g. Sardeshmukh and Hoskins (1988), Scaife et al. (2017)). Outside of the tropics, Rossby wave sources are reinforced by the Rossby waves themselves, as they result in anomalous vorticity and divergence. For this reason, we do not include any calculations of subtropical or extratropical Rossby wave source, as underestimated values in models may be caused by, rather than the cause of, underestimated teleconnection amplitude.

Figure 3 (d) shows the response of 200 hPa divergence in the tropical east Pacific (using the same box as TEP rainfall) to El Niño calculated using JRA-55, ERA5 and each model. The observational estimates have very similar mean responses. The multimodel mean is slightly weaker than observations, but it is well within the margin of uncertainty and all five individual models are within the 2 standard error range of both reanalyses. Figure 3 (e) shows the 200 hPa divergence response in the tropical west Pacific (using the box for TWP rainfall). The multimodel mean response is weaker than that of TEP divergence (around 85% of the JRA-55 response), but it is still well within the margin of error of both reanalyses. Finally, the extratropical anomalies in Figure 3 (f) demonstrate the significance of the weak response of North Pacific geopotential height to El Niño, as the strength of the multimodel mean is below the two standard error range from the JRA-55 mean. JRA-55 and ERA5 are in strong agreement on both the mean response and its error.

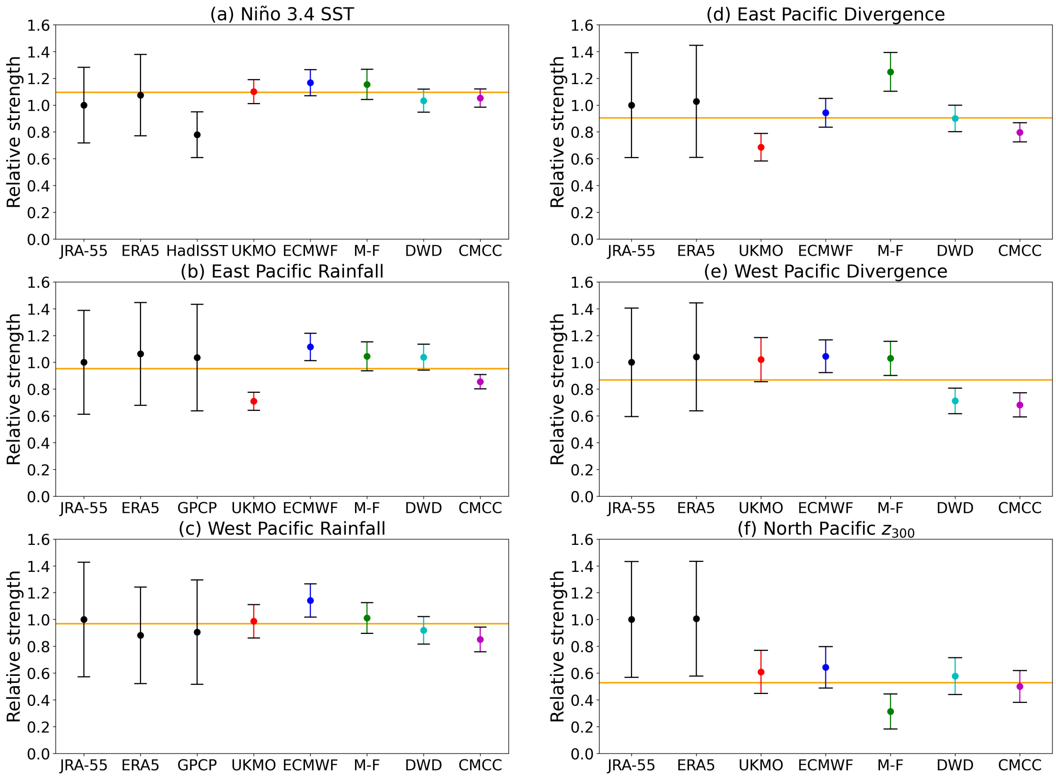

Figure 3. Strength of responses to El Niño for six indices: (a) Niño 3.4 sea surface temperature; (b) Tropical East Pacific precipitation; (c) Tropical West Pacific precipitation; (d) Tropical East Pacific divergence at 200 hPa; (e) Tropical West Pacific divergence at 300 hPa; (f) North Pacific geopotential height at 300 hPa, all normalized relative to JRA-55. Circles denote means from each data source. Error bars denote two standard errors from the mean. Orange horizontal lines denote the multimodel mean.

If it is assumed that the multimodel tropical divergence response is systematically weak, the extent to which it is weak (a factor of around 0.85 relative to JRA-55 for both TEP and TWP) is not sufficient to explain the weak North Pacific response (a factor of around 0.55) without the influence of highly non-linear mechanisms. Therefore, the tropical forcing of the teleconnection does not appear to be the source of the weak teleconnection. For La Niña we found that the TWP precipitation and divergence responses are underestimated in all models, with high significance for the multimodel mean and three of the models (ECMWF, M-F, CMCC; not shown), making it more difficult to separate tropical and extratropical effects which contribute to the underestimated teleconnection strength.

Finally, we consider the link from the Pacific to the Atlantic. Figure 4 (a) shows the geopotential height response to a unit deepening of the Aleutian Low, for JRA-55 data. Figure 4 (b) shows the same, but for the multimodel ensemble. At mid-latitudes, the geopotential height response to deepening of the Aleutian Low is relatively accurate in the multimodel ensemble — a negative NAO-like pattern (cf. Honda et al. (2001)) exists in both observations and models, and a similar dipole anomaly occurs over North America. The amplitude of the pattern is much closer to the observed link than is the case for the response to ENSO. This suggests that improving the strength of the Aleutian Low response to ENSO would improve prediction over North America and in the North Atlantic sector, as well as in the North Pacific sector. Figure 4 (c)–(g) shows the

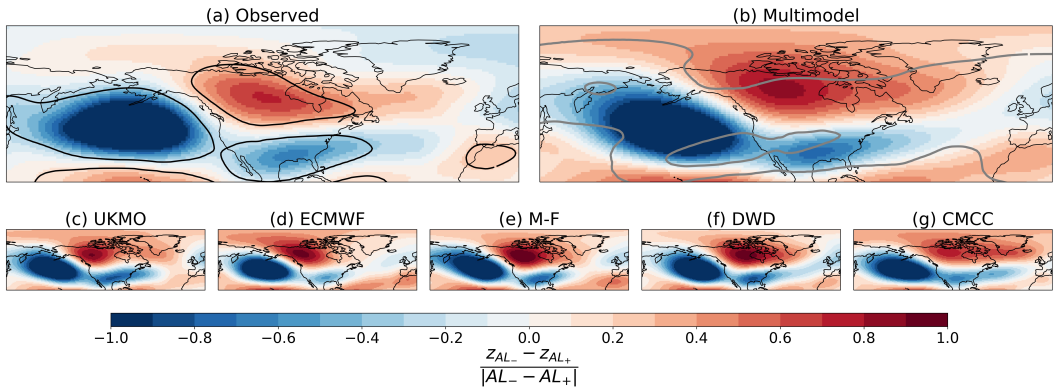

Figure 4. Teleconnections between the Pacific and Atlantic basins. 300 hPa geopotential height response to a unit deepening of the Aleutian Low. Defined as the difference between composites of geopotential height during years with a deeper-than-average Aleutian Low and those with a less deep Aleutian Low, divided by the absolute difference in the mean Aleutian Low for the same sets of years. For JRA-55 (a), the multimodel mean (b) and individual models ((c)–(g), labelled). Black line contours on (a) bound regions where the difference is significant at the 10% level in observations according to a two-tailed t test. Gray line contours on (b) bound regions where the observed and multimodel results are significantly different at the 10% level according to a two-tailed t test.

response for individual models. Each model has a similar response to the multimodel mean and observations, although they vary in how far the dipole extends eastwards into the North Atlantic, and the North Atlantic response in the ECMWF model is weaker than others.

5 Discussion and Conclusions

Underprediction of teleconnections has serious ramifications for seasonal forecasts. If total ensemble variance of forecasts is realistic, halving the strength of teleconnections will degrade model predictability and reduce skill. These results also have a bearing on the signal-to-noise paradox on interannual timescales. However, this problem is also known to exist in longer term predictions (Eade et al., 2014; Smith et al., 2020) where ENSO is not the main driver of predictable signals. Therefore, whilst ENSO is unlikely to be the direct cause of the paradox, its weak teleconnections may have the same origin, as has also been found for the Quasi-Biennial Oscillation (O'Reilly et al., 2019). It is therefore necessary to establish the cause of weak teleconnections in general, in order to not only improve modelled ENSO-associated interannual variability but potentially to also improve modelled variability due to other drivers and at different timescales. Leading hypotheses for this more general problem include transient eddy feedback (Scaife, Camp, et al., 2019; Hardiman et al., 2022) and ocean-atmosphere interaction (Zhang & Kirtman, 2019; Ossó et al., 2020). ENSO is a global driver of climate variability, but its influence on North American and European winters is underestimated in current seasonal forecasts. Solving this problem would reduce uncertainty and increase skill in winter prediction in these regions.

The underestimation of the El Niño teleconnection amplitude has strong statistical significance (cf. Figure 3 (f)) despite the uncertainty of the observed amplitude due to the limited number of observed events (cf. Deser et al. (2017)). This level of significance was found to remain when including pre-satellite era JRA-55 and ERA5 reanalysis data (starting from 1958/59 and 1950/51 respectively; not shown).

This study demonstrates that current seasonal forecasts are unable to capture the strength of the atmospheric response to ENSO in the North Pacific, which in turn affects ENSO teleconnections to the North Atlantic. This has an impact on seasonal prediction of wind speed, temperature and precipitation during winter in North America and Europe.

6 Open Research

Hindcast data from the five seasonal forecast systems used in this work are freely available online (https://doi.org/10.24381/cds.0b79e7c5 for geopotential and wind component data, and https://doi.org/10.24381/cds.68dd14c3 for all other fields), with the following originating centre and system labels: UK Met Office, 15 for UKMO; ECMWF, 5 for ECMWF; Météo France, 8 for M-F; DWD, 21 for DWD; CMCC, 35 for CMCC. Hindcast data was produced by the institutes that developed each forecast system: The UK Met Office for UKMO (MacLachlan et al., 2015); the European Centre for Medium-Range Weather Forecasts for ECMWF (Johnson et al., 2019); Météo-France for M-F (Voldoire et al., 2019); The Deutscher Wetterdienst for DWD (Fröhlich et al., 2021); The Euro-Mediterranean Center on Climate Change for CMCC (Sanna et al., 2016).

The JRA-55 reanalysis data (Kobayashi et al., 2015) used in this work are freely available online (https://doi.org/10.5065/D60G3H5B). The GPCP data (Adler et al., 2003) used in this work are freely available online (https://psl.noaa.gov/data/gridded/data.gpcp.html). The ERA5 reanalysis data (Hersbach et al., 2020) used in this work are freely available online (https://doi.org/10.24381/cds.6860a573 for geopotential and wind component data, and https://doi.org/10.24381/cds.f17050d7 for all other data). The HadISST (Kennedy et al., 2017) sea surface temperature data used in this work is freely available online at https://esgf-node.llnl.gov/search/input4mips/ under the HighResMIP (Haarsma et al., 2016) Target MIP.

Acknowledgments

N.C.W. was supported by a NERC GW4+ Doctoral Training Partnership studentship from the Natural Environment Research Council (NE/L002434/1). A.A.S. was supported by the Met Office Hadley Centre Climate Programme funded by BEIS and the Natural Environment Research Council NE/S004645/1.

References

Abid, M. A., Kucharski, F., Molteni, F., Kang, I.-S., Tompkins, A. M., & Almazroui, M. (2021). Separating the Indian and Pacific Ocean impacts on the Euro-Atlantic response to ENSO and its transition from early to late winter. *Journal of Climate*, *34*(4), 1531–1548.

Adler, R. F., Huffman, G. J., Chang, A., Ferraro, R., Xie, P.-P., Janowiak, J., ... Nelkin, E. (2003). The version-2 global precipitation climatology project (GPCP) monthly precipitation analysis (1979–present). *Journal of Hydrometeorology*, *4*(6), 1147–1167. Retrieved from `https://doi.org/10.1175/1525-7541(2003)004<1147:TVGPCP>2.0.CO;2`

Ayarzagüena, B., Ineson, S., Dunstone, N. J., Baldwin, M. P., & Scaife, A. A. (2018). Intraseasonal effects of El Niño–Southern Oscillation on North Atlantic Climate. *Journal of Climate*, *31*(21), 8861–8873.

Baker, L., Shaffrey, L., Sutton, R., Weisheimer, A., & Scaife, A. A. (2018). An intercomparison of skill and overconfidence/underconfidence of the wintertime North Atlantic Oscillation in multimodel seasonal forecasts. *Geophysical Research Letters*, *45*(15), 7808–7817.

Bladé, I., Newman, M., Alexander, M. A., & Scott, J. D. (2008). The late fall extratropical response to ENSO: sensitivity to coupling and convection in the tropical West Pacific. *Journal of Climate*, *21*(23), 6101–6118.

Cagnazzo, C., & Manzini, E. (2009). Impact of the stratosphere on the winter tropospheric teleconnections between ENSO and the North Atlantic and European region. *Journal of climate*, *22*(5), 1223–1238.

Deser, C., Simpson, I. R., McKinnon, K. A., & Phillips, A. S. (2017). The Northern Hemisphere extratropical atmospheric circulation response to ENSO: How well do we know it and how do we evaluate models accordingly? *Journal of Climate*, *30*(13), 5059–5082.

Eade, R., Smith, D. M., Scaife, A. A., Wallace, E., Dunstone, N. J., Hermanson, L., & Robinson, N. (2014). Do seasonal-to-decadal climate predictions underestimate the predictability of the real world? *Geophysical Research Letters*, *41*(15), 5620–5628.

Fröhlich, K., Dobrynin, M., Isensee, K., Gessner, C., Paxian, A., Pohlmann, H., ... Baehr, J. (2021). The German climate forecast system: GCFS. *Journal of Advances in Modeling Earth Systems*, *13*(2), e2020MS002101. Retrieved from `https://doi.org/10.1029/2020MS002101`

Haarsma, R. J., Roberts, M. J., Vidale, P. L., Senior, C. A., Bellucci, A., Bao, Q., ... von Storch, J.-S. (2016). High resolution model intercomparison project (HighResMIP v1. 0) for CMIP6. *Geoscientific Model Development*, *9*(11), 4185–4208.

Hardiman, S. C., Dunstone, N. J., Scaife, A. A., Smith, D. M., Comer, R., Nie, Y., & Ren, H.-L. (2022). Missing eddy feedback may explain weak signal-to-noise ratios in climate predictions. *npj Climate and Atmospheric Science*, *5*(57).

Hersbach, H., Bell, B., Berrisford, P., Hirahara, S., Horányi, A., Muñoz-Sabater, J., ... Thépaut, J.-N. (2020). The ERA5 global reanalysis. *Quarterly Journal of the Royal Meteorological Society*, *146*(730), 1999–2049. Retrieved from `https://doi.org/10.1002/qj.3803`

Honda, M., Nakamura, H., Ukita, J., Kousaka, I., & Takeuchi, K. (2001). Interannual seesaw between the Aleutian and Icelandic lows. Part I: Seasonal dependence and life cycle. *Journal of Climate*, *14*(6), 1029–1042.

Horel, J. D., & Wallace, J. M. (1981). Planetary-scale atmospheric phenomena associated with the Southern Oscillation. *Monthly Weather Review*, *109*(4), 813–829.

Ineson, S., & Scaife, A. A. (2009). The role of the stratosphere in the European climate response to El Niño. *Nature Geoscience*, *2*(1), 32–36.

Johnson, S. J., Stockdale, T. N., Ferranti, L., Balmaseda, M. A., Molteni, F., Magnusson, L., … Monge-Sanz, B. M. (2019). SEAS5: the new ECMWF seasonal forecast system. *Geoscientific Model Development*, *12*(3), 1087–1117. Retrieved from https://doi.org/10.5194/gmd-12-1087-2019

Kennedy, J., Titchner, H., Rayner, N., & Roberts, M. (2017). input4MIPs. MOHC. SSTsAndSeaIce. HighResMIP. MOHC-HadISST-2-2-0-0-0. Version 20170505. *Earth System Grid Federation*, *10*. Retrieved from https://esgf-node.llnl.gov/search/input4mips

Kobayashi, S., Ota, Y., Harada, Y., Ebita, A., Moriya, M., Onoda, H., … Takahashi, K. (2015). The JRA-55 reanalysis: General specifications and basic characteristics. *Journal of the Meteorological Society of Japan. Ser. II*, *93*(1), 5–48. Retrieved from https://doi.org/10.2151/jmsj.2015-001

Kucharski, F., Molteni, F., & Bracco, A. (2006). Decadal interactions between the western tropical Pacific and the North Atlantic Oscillation. *Climate Dynamics*, *26*(1), 79–91.

L'Heureux, M. L., Tippett, M. K., Kumar, A., Butler, A. H., Ciasto, L. M., Ding, Q., … Johnson, N. C. (2017). Strong relations between ENSO and the Arctic Oscillation in the North American multimodel ensemble. *Geophysical Research Letters*, *44*(22), 11–654.

MacLachlan, C., Arribas, A., Peterson, K. A., Maidens, A., Fereday, D., Scaife, A., … Madec, G. (2015). Global Seasonal forecast system version 5 (GloSea5): A high-resolution seasonal forecast system. *Quarterly Journal of the Royal Meteorological Society*, *141*(689), 1072–1084. Retrieved from https://doi.org/10.1002/qj.2396

Moron, V., & Gouirand, I. (2003). Seasonal modulation of the El Niño–Southern Oscillation relationship with sea level pressure anomalies over the North Atlantic in October–March 1873–1996. *International Journal of Climatology: A Journal of the Royal Meteorological Society*, *23*(2), 143–155.

O'Reilly, C. H., Weisheimer, A., Woollings, T., Gray, L. J., & MacLeod, D. (2019). The importance of stratospheric initial conditions for winter North Atlantic Oscillation predictability and implications for the signal-to-noise paradox. *Quarterly Journal of the Royal Meteorological Society*, *145*(718), 131–146.

Ossó, A., Sutton, R. T., Shaffrey, L. C., & Dong, B. (2020). Development, amplification, and decay of Atlantic/European summer weather patterns linked to spring North Atlantic sea surface temperatures. *Journal of Climate*, *33*(14), 5939–5951.

Sanna, A., Borrelli, A., Athanasiadis, P., Materia, S., Storto, A., Navarra, A., … Gualdi, S. (2016). CMCC-SPS3: the CMCC Seasonal Prediction System 3. *CMCC Research Paper*(RP0285). Retrieved from https://www.cmcc.it/publications/rp0285-cmcc-sps3-the-cmcc-seasonal-prediction-system-3

Sardeshmukh, P. D., & Hoskins, B. J. (1988). The generation of global rotational flow by steady idealized tropical divergence. *Journal of the Atmospheric Sciences*, *45*(7), 1228–1251.

Scaife, A. A., Arribas, A., Blockley, E., Brookshaw, A., Clark, R., Dunstone, N. J., … Williams, A. (2014). Skillful long-range prediction of European and North American winters. *Geophysical Research Letters*, *41*(7), 2514–2519.

Scaife, A. A., Camp, J., Comer, R. E., Davis, P., Dunstone, N. J., Gordon, M., … Vidale, P. L. (2019). Does increased atmospheric resolution improve seasonal climate predictions? *Atmospheric Science Letters*, *20*(8), e922.

Scaife, A. A., Comer, R. E., Dunstone, N. J., Knight, J. R., Smith, D. M., MacLachlan, C., … Slingo, J. (2017). Tropical rainfall, Rossby waves and regional winter climate predictions. *Quarterly Journal of the Royal Meteorological Society*, *143*(702), 1–11.

Scaife, A. A., Ferranti, L., Alves, O., Athanasiadis, P., Baehr, J., Dequé, M., …

Yang, X. (2019). Tropical rainfall predictions from multiple seasonal forecast systems. *International Journal of Climatology*, *39*(2), 974–988.
Scaife, A. A., & Smith, D. M. (2018). A signal-to-noise paradox in climate science. *npj Climate and Atmospheric Science*, *1*(1), 1–8.
Smith, D. M., Scaife, A. A., Eade, R., Athanasiadis, P., Bellucci, A., Bethke, I., ... Zhang, L. (2020). North Atlantic climate far more predictable than models imply. *Nature*, *583*(7818), 796–800.
Toniazzo, T., & Scaife, A. A. (2006). The influence of ENSO on winter North Atlantic climate. *Geophysical Research Letters*, *33*(24).
Trenberth, K. E. (1997). The definition of El Niño. *Bulletin of the American Meteorological Society*, *78*(12), 2771–2778.
Voldoire, A., Saint-Martin, D., Sénési, S., Decharme, B., Alias, A., Chevallier, M., ... Waldman, R. (2019). Evaluation of CMIP6 deck experiments with CNRM-CM6-1. *Journal of Advances in Modeling Earth Systems*, *11*(7), 2177–2213. Retrieved from `https://doi.org/10.1029/2019MS001683`
Zhang, W., & Kirtman, B. (2019). Understanding the signal-to-noise paradox with a simple Markov model. *Geophysical Research Letters*, *46*(22), 13308–13317.

Supporting Information for ”Underpredicted ENSO Teleconnections in Seasonal Forecasts”

N. C. Williams[1], A. A. Scaife[1,2], and J. A. Screen[1]

[1]College of Engineering, Mathematics and Physical Sciences, University of Exeter, Exeter, UK

[2]Met Office Hadley Centre, Exeter, UK

Contents of this file

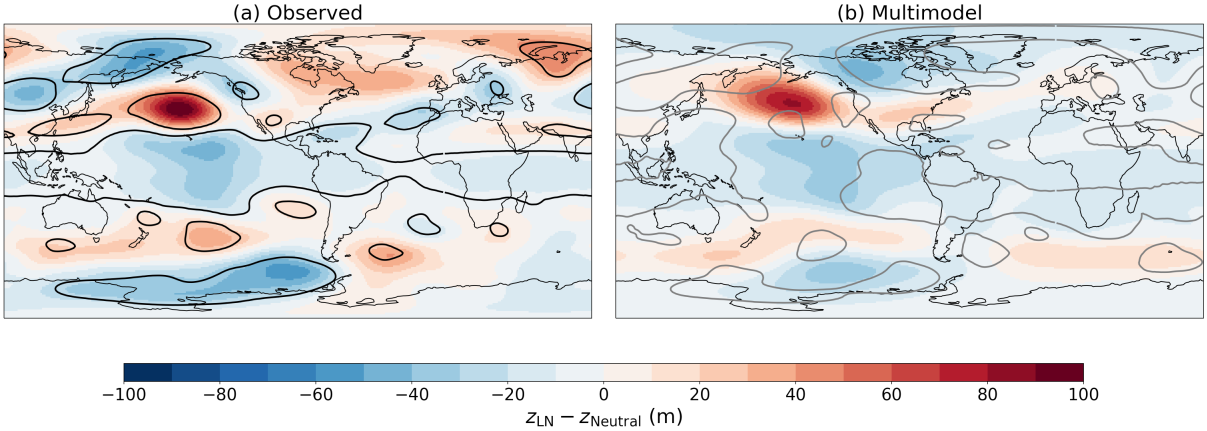

Figure S1. Geopotential height response to La Niña. Difference between La Niña and neutral composites of 300 hPa geopotential height for JRA-55 (a) and the mean of all five models (b). Black line contours on (a) bound regions where the La Niña and neutral years are significantly different above the 10% level in observations according to a two-tailed t test. Gray line contours on (b) bound regions where the modelled response is significantly different to the observed response at the 10% level according to a two-tailed t test.